Sol Gel Synthesis of $Li_{1+\alpha}V_3O_8$. 1. From Precursors to Xerogel

Matthieu Dubarry,[†] Joël Gaubicher,*[,†] Dominique Guyomard,[†] Olivier Durupthy,[‡] Nathalie Steunou,[‡] Jacques Livage,[‡] Nicolas Dupré,[§] and Clare P. Grey[§]

Institut des Matériaux Jean Rouxel, 2 rue de la Houssinière, BP 32229, 44322 Nantes Cedex 3, France, Laboratoire de Chimie de la Matière Condensée, Université Pierre et Marie Curie-Paris VI, 4 place Jussieu, 75252 Paris Cedex 05, France, and SUNY, Stony Brook University, Stony Brook, New York 11794-3400

Received December 10, 2004. Revised Manuscript Received March 3, 2005

The nature of $Li_{1+\alpha}V_3O_8 \cdot nH_2O$ gel-like precipitate and corresponding xerogels has been studied. Unlike V_2O_5 gel, the $Li_{1+\alpha}V_3O_8$ gels are diphasic materials made of intimately mixed solid and liquid phases having very close Li/V stoichiometry. At room temperature, the solid component contains presumably an hewettite type structure, whereas the liquid part crystallizes into lithiated decavanadic acids. Upon drying at 90 °C, both components lead to hydrated $Li_{1+\alpha}V_3O_8 \cdot nH_2O$ hewettite-like compounds with different interlayer spacing but with the same water content. By coupling pH measurements, X-ray diffraction, and liquid and magic-angle spinning ^{51}V NMR, a new mechanism of formation of the $Li_{1+\alpha}V_3O_8$ gel-like precipitate via solubilized vanadic species is proposed.

Introduction

Lithium vanadium oxide, $Li_{1+\alpha}V_3O_8$ ($\alpha = 0.1-0.2$) has been extensively studied during the past 20 years for its attractive electrochemical properties in rechargeable lithium batteries.[1−3] It provides a fair energy density and a good capacity retention.[4,5] Two routes have been mainly used to synthesize these oxides: solid-state reactions[2,3,5] and sol−gel syntheses.[4,6] The lithium insertion behavior of $Li_{1+\alpha}V_3O_8$ strongly depends on the firing temperature of the xerogel.[4−6,7] Samples prepared upon heating at 580 °C exhibit a stable capacity of 180 mAh/g upon cycling,[5] whereas those heated at 350 °C, which can only be prepared using a sol−gel route, exhibit a larger initial capacity (300 mAh/g) that decreases rapidly upon cycling.[5,7] Understanding the chemical nature of the gel precursor and the chemical processes that lead from the gel to $Li_{1+\alpha}V_3O_8$ oxide might suggest new approaches for improving its electrochemical properties.

In the sol−gel synthesis, a gel-like intermediate is prepared via the condensation of solute precursors in aqueous solution. Gelation of the $Li_{1+\alpha}V_3O_8$ precursor is obtained upon reaction of V_2O_5 with a stoechiometric amount of $LiOH \cdot H_2O$ in water at 50 °C under nitrogen after 24−36 hours.[1−3] A mechanism involving solid-state reactions has been proposed

$$6LiOH,H_2O + V_2O_5 \rightarrow 2Li_3VO_4 + 9H_2O \quad (1)$$

$$Li_3VO_4 + V_2O_5 \rightarrow 3LiVO_3 \quad (2)$$

$$LiVO_3 + V_2O_5 \rightarrow LiV_3O_8 \quad (3)$$

The obtained xerogel has been described as a poorly crystallized layered hydrate $Li_{1+\alpha}V_3O_8 \cdot nH_2O$. The chemical nature of the gel and the xerogel has never been studied. They were assumed to be single-phase materials. Very close materials were also obtained via reaction of $Li_{1+\alpha}V_3O_8$ in water.[8−10] According to the drying procedure, different hydrated phases (related to different interlayer distances)[10] or even mixed phases[4,9] were obtained. Neither the structure nor the water content of these xerogels or hydrates has been carefully characterized.

The goal of the present study is to clarify these points as well as to propose a new mechanism of the $Li_{1+\alpha}V_3O_8$ gel formation via solubilized vanadium species.

Experimental Section

$Li_{1+\alpha}V_3O_8$ gels have been prepared as described in the literature.[1−3] $LiOH \cdot H_2O$ powder was reacted with a suspension of α-V_2O_5 (Aldrich 99.6%) in distilled water at 50 °C under N_2 atmosphere for 30 h. The α-V_2O_5 concentration has been varied from 0.35 $mol \cdot L^{-1}$ to 3 $mol \cdot L^{-1}$ in order to assess its influence on the final product. Solid-state reacted $Li_{1.1}V_3O_8$ (ss-$Li_{1.1}V_3O_8$) was prepared by firing at 580 °C for 10 h a stoichiometric mixture of α-V_2O_5 and Li_2CO_3 in a platinium crucible. V_2O_5 gel was prepared by reacting 1 g of α-V_2O_5 in 30 mL of H_2O_2 30%. pH measurements

* To whom correspondence should be addressed. E-mail: joel.gaubicher@cnrs-imn.fr. Tel: 0033 2 40 37 39 32. Fax: 0033 2 40 37 39 95.
[†] Institut des Materiaux Jean Rouxel.
[‡] Universite Pierre et Marie Curie.
[§] SUNY, Stony Brook University.

(1) Guyomard, D. In *New Trends in Electrochemical Technology: Energy Storage Systems in Electronics*; Osaka, T., Matta, D., Eds.; Gordon & Breach, Philadelphia, 2000; Chapter 9, p 253.
(2) Nassau, K.; Murphy, D. W. *J. Non-Cryst. Solids* **1981**, *44*, 297.
(3) Pistoia, G.; Panero, S.; Tocci, M.; Moshtev, R. V.; Manev, V. *Solid State Ionics* **1984**, *13*, 311.
(4) West, K.; Zachau-Christainsen, B.; Skaarup, S.; Saidi, M. Y.; Barker, J.; Olsen, I. I.; Pynenburg, R.; Koksbang, R. *J. Electrochem. Soc.* **1996**, *143*, 820.
(5) Jouanneau, S.; Le Gal La Salle, A.; Verbaere, A.; Guyomard, D.; Deschamps, M.; Lascaud, S. *Solid State Ionics*, in press.
(6) Pistoia, G.; Pasquali, M.; Wang, G.; Li, L. *J. Electrochem. Soc.* **1990**, *137*, 2365.
(7) Jouanneau, S.; Le Gal La Salle, A.; Verbaere, A.; Deschamps, M.; Lascaud, S.; Guyomard, D. *J. Mater. Chem.* **2003**, *13*, 921.
(8) Schöllhorn, R.; Klein-Reesink, F.; Reimold, R. *J. Chem. Soc. Chem. Commun.* **1979**, 398.
(9) Manev, V.; Momchilov, A.; Nassalevska, A.; Pistoia, G.; Pasquali, M. *J. Power Sources* **1995**, *54*, 501.
(10) Kumagai, N.; Yu, A. *J. Electrochem. Soc.* **1997**, *144*, 830.

10.1021/cm047845k CCC: $30.25
Published on Web 03/30/2005

were performed with a pH meter using 2 points (4 and 7) for calibration. The centrifugations were performed at 6400 tr/min for 5 min. X-ray diffraction (XRD) data were collected with a Θ/2Θ SIEMENS D5000 diffractometer with a linear MOXTEK detector and thermodiffractometry on a Θ/Θ SIEMENS D5000 diffractometer mounted with a PSD detector. Synchrotron experiments were performed at ESRF (Grenoble, France) on a BM01B beam line. For XRD of room-temperature xerogels, gels or liquids were casted on a polish glass substrate and dried at room temperature before any heat treatment.

Solution ^{51}V NMR spectra were recorded at 105.2 MHz on a Bruker Advance 400 spectrometer. The chemical shifts were measured relative to the external standard $VOCl_3$ at 0 ppm. Transients (128 or 256) were accumulated at 323 K. We typically used a spectral width of 31447 Hz, a pulse width of 17μs ($\sim\theta-90°$), an accumulation time of 500 ms, and no relaxation delay.

^{51}V magic-angle spinning (MAS) NMR experiments were performed at the operating frequencies of 94.69 and 52.61 MHz, on CMX-360 and CMX-200 spectrometers, corresponding to field strengths of 8.4 and 4.7 T, respectively. Spectra were acquired with a single-pulse sequence or a rotor-synchronized (π/12-τ-π/6-τ-acq.) echo sequence where $\tau = 1/\nu_r$ and ν_r is the spinning frequency. π/12 pulse widths of 1 μs and pulse delays of 0.5 s were used. A Chemagnetics probe equipped with a 3.2-mm rotor was used, with typical spinning frequencies of 15 and 20 kHz, to determine the frequency of the isotropic resonances. Spectra at 30 kHz were acquired using a probe equipped with a 2-mm rotor. ^{51}V spectra were referenced to 1 M solution $VOCl_3$ as an external reference. High-temperature spectra acquisition was achieved using a Chemagnetics variable temperature stack and controller. A lower spinning speed of 15 kHz was used in order to minimize the temperature gradient between the sample and the thermocouple. Spectra deconvolutions and intensities integration were performed using the NUTS software. The SIMPSON program[11] was used to simulate ^{51}V spectra, including satellite transitions, first-, and second-order quadrupolar interactions. No least-squares fitting were performed due to the broad line widths and the severe overlap of the resonances.

Scanning electron microscopy (SEM) images were obtained from a GEOL 6400 microscope. Thermogravimetric analysis (TGA) experiments were performed on a SETARAM TG-DSC 111 apparatus under air flow.

Results

$Li_{1+\alpha}V_3O_8$ gels have been prepared from different precursor concentrations keeping a [V]/[Li] = 2.73 stoichiometric ratio corresponding to the stoichiometry 1.1 Li/3 V. $Li_{1+\alpha}V_3O_8$ gels or precipitates can be obtained depending on initial concentrations: below [Li] = 0.275 mol·L^{-1} precipitation occurs, whereas gels are obtained for 0.275 mol·L^{-1} < [Li] < 2.2 mol·L^{-1}. A highly viscous paste is obtained for [Li] > 2.2 mol·L^{-1}. In the gel domain of concentration, the reaction time decreases from 25 to 10 h when the Li concentration is increased from 1.5 to 2.2 mol·L^{-1}. It has to be noted that, from a mechanical point of view, $Li_{1+\alpha}V_3O_8$ gel is easier to centrifugate than V_2O_5 gel. For this reason, $Li_{1+\alpha}V_3O_8$ gels should be considered as being gel-like precipitates (GP).

The pH variation for [$LiOH·H_2O$] = 1.65 mol·L^{-1} is reported in Figure 1. The initial pH value is close to 2.5 as

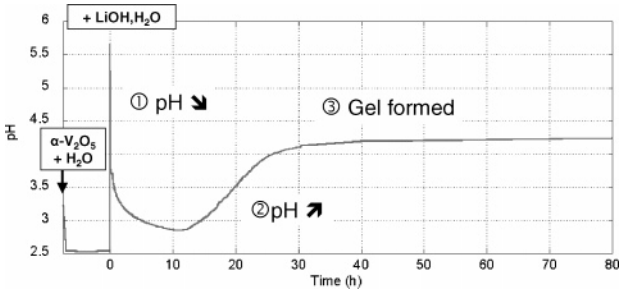

Figure 1. pH variation during the formation of the $Li_{1.1}V_3O_8$ gelatinous precipitate ([V_2O_5] = 2.25 M, [$LiOH·H_2O$] = 1.65 M).

a slight dissolution of α-V_2O_5 occurs. Upon addition of $LiOH·H_2O$, a sharp increase of the pH value up to 5.5 is observed before it decreases down to 2.8 in 12 h. At this point, the orange suspension turns brown/red and a gelatinous precipitate of the same color gradually forms along with an increase of the pH up to 4.25 after 30 h.

To get an insight of the condensation mechanism that leads to the gelatinous precipitate, both in situ ^{51}V NMR and XRD of samples extracted at different stages of the reaction were undertaken. Solution ^{51}V NMR should be a useful technique as polyoxovanadates species have already been extensively studied.[12−15]

The relative concentrations of different soluble vanadic species derived from the NMR signals are presented in Figure 2. The slight dissolution of V_2O_5 occurs upon reaction 4 as $[VO_2]^+$ and decavanadic acid $[H_2V_{10}O_{28}]^{4-}$ species are detected before the addition of $LiOH·H_2O$ ($t = -1$ min) (Figure 2a). At $t = 0$, upon addition of $LiOH·H_2O$, the pH increases immediately up to 5.5 and deprotonated decavanadic acid species $[HV_{10}O_{28}]^{5-}$ appear at the expense of the $[VO_2]^+$ and $[H_2V_{10}O_{28}]^{4-}$ species (Figure 2a). Simultaneously, dissolution of α-V_2O_5 mainly results in the formation of cyclic metavanadate $[V_4O_{12}]^{4-}$ as expected in this pH range (reaction 5)

$$6\alpha\text{-}V_2O_5 + 2OH^- \rightarrow 2[VO_2]^+ + [H_2V_{10}O_{28}]^{4-} \quad (4)$$

$$2\alpha\text{-}V_2O_5 + 4OH^- \rightarrow [V_4O_{12}]^{4-} + 2H_2O \quad (5)$$

The consumption of OH^-, corresponding to reaction 5 and the dissolution of α-V_2O_5, account for the rapid decrease of the pH. $[V_4O_{12}]^{4-}$ species that are no more stable for pH < 6 transform to $[HV_{10}O_{28}]^{5-}$ species according to reaction 6 (parts a and b of Figure 2). Acidification of the solution also leads to protonation of $[HV_{10}O_{28}]^{5-}$ in $[H_2V_{10}O_{28}]$.[4−8] Both reactions slow the decrease of the pH (between $t = 30$ min and 7 h and 30 min).

$$5[V_4O_{12}]^{4-} + 10H_3O^+ \rightarrow 2[HV_{10}O_{28}]^{5-} + 14H_2O \quad (6)$$

The pH increase stems from the condensation mechanism of the gel which is associated with proton consumption and the formation of the neutral precursor $[VO(OH)_3]^0$ (reaction 7) as in V_2O_5 gels.[16] Note that during the gelification process

(11) Baks, M.; Rasmussen, J. T.; Nielsen, N. C. *J. Magn. Res.* **2000**, *147* (2), 296.
(12) Levanto, U. *Acta Polytech. Scand.* **1969**, *82*, 7.
(13) Heath, E.; Howarth, O. *J. Chem. Soc., Dalton Trans.* **1981**, 1105.
(14) Howarth, O.; Jarrold, M. *J. Chem. Soc., Dalton Trans.* **1978**, 503.
(15) Alonso, B.; Livage, J. *J. Solid-State Chem.* **1999**, *148*, 16.
(16) Livage, J. *Chem. Mater.* **1991**, *3*, 578.

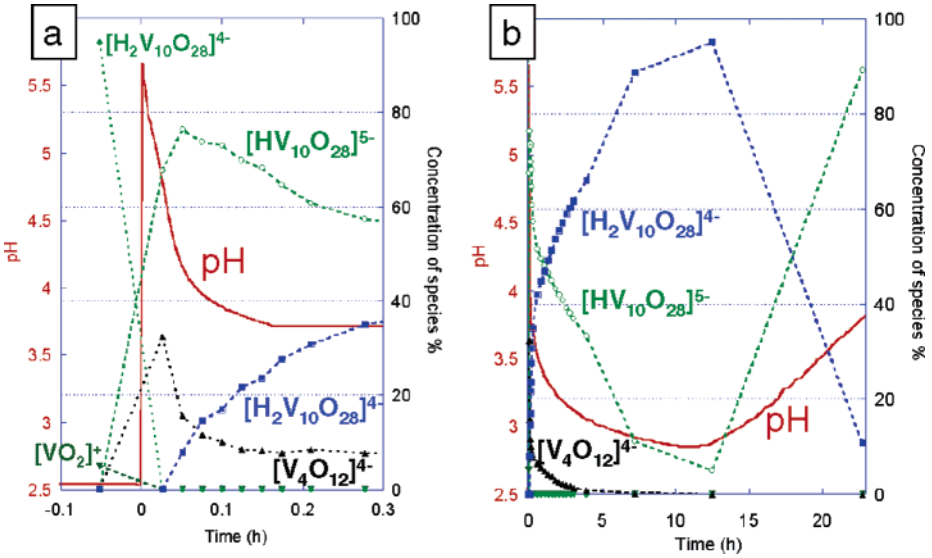

Figure 2. (a and b) Evolution of the proportion of the different vanadic species that appear during the $Li_{1+\alpha}V_3O_8$ gelification reaction.

$[VO_2]^+$ species were not observed so that they should not be involved as often proposed for V_2O_5 gels.[16]

$$[H_xV_{10}O_{28}]^{(5-x)-} + (5-x)H_3O^+ + (7+x)H_2O \rightarrow [H_6V_{10}O_{28}]^0 + 12H_2O \rightarrow 10[VO(OH)_3]^0 \quad (7)$$

As inferred from peak integration, the vanadium concentration in the solution is constant during the complete dissolution of α-V_2O_5 so that the condensation mechanism occurs simultaneously with the dissolution of α-V_2O_5.

XRD patterns were collected at selected stages of the reaction (noted ① at $t_1 = -1$ min, ② at $t_2 = 6$ min, and ③ at $t_3 = 8$ h and 30 min where $t = 0$ corresponds to the addition of $LiOH{\cdot}H_2O$). Samples extracted from the reacting medium were centrifugated. The liquid part (called D-LC_{90} for dried liquid component at 90 °C) was dropped on an appropriate X-ray holder and dried at 90 °C overnight, whereas the centrifuged solid (called D-SC_{90} for dried solid component at 90 °C) was washed with alcohol prior to drying. Corresponding XRD patterns are reported in Figure 3. Upon heating at 580 °C for 10 h, both samples D-SC_{90} and D-LC_{90} give pure $Li_{1+\alpha}V_3O_8$ ($0.1 < \alpha < 0.2$).

In regard to the solid part, XRD analysis shows that the pristine α-V_2O_5 has totally reacted in less than 8 h after the $LiOH{\cdot}H_2O$ addition. The final product is poorly crystallized and gives rise to a major line at $2\theta = 9.5°$ as well as a hump in the background between $2\theta = 25$ and 35°. For the liquid part, at least two compounds have crystallized in ②, one of them being the final product observed in ③. The other peaks (+) that could not be indexed so far might correspond to precipitates from Li^+ ions and $[V_4O_{12}]^{4-}$ species that are observed from NMR. The diagram of the main phase is similar to that obtained from the solid part except for the most intense line that appears at higher angles ($2\theta = 10.5°$). Crystallized $LiVO_3$ or Li_3VO_4 were not observed however during the reaction, as expected from the literature, although they, or their hydrated phases, can be obtained in close conditions. For instance, $LiVO_3$ could be obtained using a 3× times excess of lithium ions.

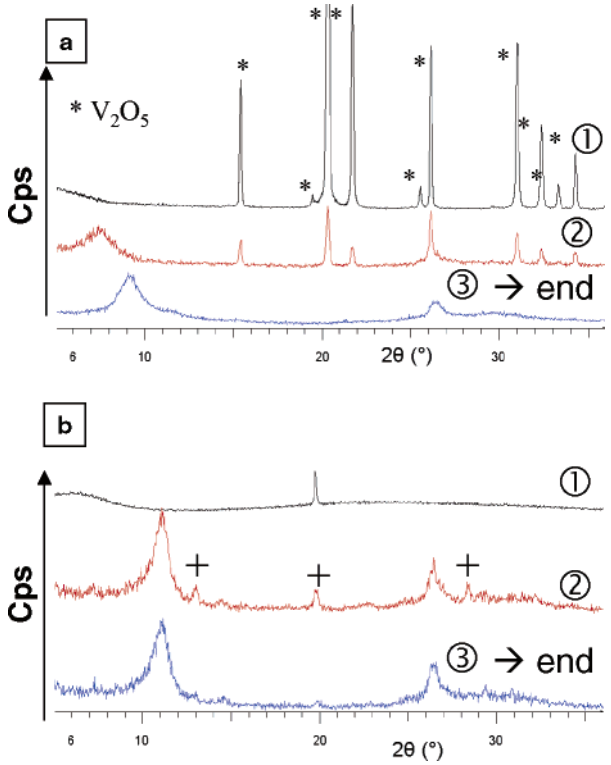

Figure 3. XRD (Cu Kα) patterns evolution for samples extracted during the gelification reaction (a) for the solid component (D-SC_{90}), (b) for the liquid component (D-LC_{90}) in the case of extraction at ①, $t = -1$ min; ②, $t = 6$ min; and ③ 8 h and 30 min $< t <$ 30 h.

The X-ray diagram obtained from the gelatinous precipitate dried at 90 °C shows that the xerogel (X_{90}) is a diphasic compound (Figure 4), each phase coming from the liquid and solid components (D-LC_{90}) and (D-SC_{90}). Moreover if the gel is aged 9 months and dried at 90 °C (labeled AG_{90}) or if $Li_{1+\alpha}V_3O_8$ is dissolved in water and recrystallized at 90 °C, the obtained diffraction patterns contain sharper reflections similar angular positions to that of D-LC_{90}. XRD pattern of the former is reported in Figure 4.

By use of synchrotron radiation at ESRF, the AG_{90} diffractogram could be indexed using Dicvol software[17] in a monoclinic system with $a = 15.57$ Å, $b = 7.16$ Å, $c = 12.14$ Å, and $\beta = 91.70$ (1)°. From space group solutions proposed

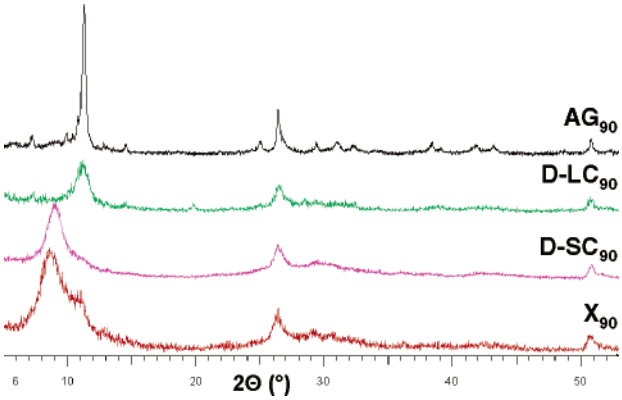

Figure 4. XRD (Cu Kα) patterns of a $Li_{1.1}V_3O_8$ GP (X_{90}), its solid component (D-SC_{90}), its liquid component (D-LC_{90}), and 9 months aged GP dried overnight at 90 °C (AG_{90}).

by Checkcell software,[18] the best space group was found to be $P2_1/m$. The corresponding profile matching refinement using Fullprof software[19] lead to good reliability factors (R_{wp} = 6.3% and R_{exp} = 5.2%) and a = 15.5719 (3) Å, b = 7.1676 (1) Å, c = 12.1413 (3) Å, and β = 91.708 (1)°. The observed and calculated patterns as well as the difference curves are reported in Figure 5. These results show close similarities with the metrics of lamellar hewettite compounds such as $Na_2V_6O_{16}\cdot 3H_2O$ that contain the same $V_3O_8^{(1+\alpha)-}$ layers that are in $Li_{1+\alpha}V_3O_8$. Indeed these compounds mainly crystallize in $P2_1/m$ space group with b_0 close to 3.6 Å and c close to 12 Å. In our case, however, a superstructure along a and b is observed ($a = 2a_0$ and $b = 2b_0$). Such a superstructure has already been observed in other hewettite compounds.[20] The structural determination is underway. TGA measurements show that this compound contains 1 mole of water per formula unit. It will be called LVOH1 for $Li_{1+\alpha}V_3O_8\cdot H_2O$.

In light of these results and as inferred from Figure 4, each of the GP components is related to a hewettite-like compound but with different interlayer spacing: LVOH1 for D-LC_{90} and another phase, called LVOH2, with a larger interlayer space for the D-SC_{90} (Figure 4). They contain similar lithium contents, as both of them give pure $Li_{1+\alpha}V_3O_8$ ($0.1 < \alpha < 0.2$) phase upon firing above 250 °C. TGA measurements show that they both contain a similar amount of water, i.e., 1.1 mol per formula unit so that the two distinct interlayer distances observed for LVOH1 and LVOH2 could stem from a different water molecule organization within the interlayer space. This could be related to the number of water molecules in the hydration sphere of Li^+ ions. A similar hypothesis has been mentioned in a previous study by Baffier et al.[21] for $A_xV_2O_5\cdot nH_2O$. Moreover, as for AG_{90} the only phase observed upon drying X_{90} for one month at 90 °C is LVOH1; LVOH2 is metastable. This presumably comes from a low kinetics of the water molecule reorganization.

As a conclusion, the $Li_{1.1}V_3O_8$ xerogel prepared at 90 °C is a diphasic compound composed of two different hewettite-like compounds LVOH1 and LVOH2 that presumably differ from water position within the interlayer space. To determine the origin of this diphasic nature, a similar study was undertaken with xerogels prepared at room temperature.

The diffraction patterns of (a) the xerogel X_{25}, (b) its liquid component D-LC_{25}, and (c) its solid component D-SC_{25} separated by centrifugation and dried at room temperature are presented in Figure 6. The biphasic character of the xerogel is even more pronounced at room temperature. Indeed, it appears as being composed of two very different components, D-SC_{25} that is already a hewettite-like compound and D-LC_{25} that is characterized by much thinner peaks. ^{51}V liquid NMR results showed that decavanadate is the only vanadium species present with lithium counterions when the gel forms. D-LC_{25} should thus correspond to one or several lithium decavanadates that have precipitated. Such crystallized decavanadic acids with alkali counterions are well known, especially with Na^+ ions, but none have been reported to our knowledge with Li^+ ions.

D-SC_{25} shows a larger interlayer space than LVOH2. TGA measurements indicate that it contains about 3 times more water molecules than LVOH2 and LVOH1. It will be noted LVOH3.

To probe the local environment of the vanadium ions, ^{51}V MAS NMR spectroscopy has been performed on these three samples (Figure 7). The spectra obtained from room-temperature experiments on D-LC_{25}, D-SC_{25}, and X_{25} (Figure 7a) contain very broad resonances that can be attributed to a chemical shift distribution, indicating a distribution in the local environments of the lithium ions/V atoms. Three main types of resonances are observed in both echo and single-pulse spectra for D-SC_{25}, at −545, −580, and −610 ppm indicating that there are at least three different local environments for vanadium. Signals at approximately −580 and −610 ppm have been observed in ^{51}V NMR spectra of layered xerogel $V_2O_5\cdot nH_2O$ (Figure 7b)[22] and can be attributed to pentacoordinated V^V ions with a vanadyl bond. The main resonance at −545 ppm for the D-SC_{25} sample has not been observed previously and thus corresponds to local environment(s) completely different from those within the V_2O_5 gel. The ^{51}V MAS NMR spectrum of $Li_{1.1}V_3O_8$ is shown in Figure 7b. The deconvolution and integration of the resonances, including the spinning sidebands, indicated the presence of three distinct signals at approximately −535, −550, and −575 ppm. The structure of $Li_{1.1}V_3O_8$ is composed of two octahedral and one pentacoordinated vanadium ions.[23] The resonance at −575 ppm has been attributed to the pentacoordinated environment on the basis of a larger quadrupolar coupling constant[24] (C_Q = 1 MHz) in comparison of that of the two other (Q_{cc} = 0.8 MHz). Large values of the asymmetry parameters (η_Q= 0.5 and 0.9 for the octahedral and pentacoordinated sites, respectively)

(17) Boultif, A.; Lauër, D. *J. Appl. Crystallogr.* **1991**, *24*, 987.
(18) Laugier, J.; Bochu, B. Laboratoire des Matériaux et du Génie Physique Grenoble.
(19) Roisnel, T.; Carvajal, R. *Mater. Sci. Forum* **2001**, *118*, 378−381.
(20) Oka, Y. et al. *J. Solid-State Chem.* **1998**, *140*, 219.
(21) Bouhaouss, A.; Aldebert, P.; Baffier, N.; Livage, J. *Rev. Chim. Miner.* **1985**, *22*, 417.
(22) Fontenot, C. J.; Wiench, J. W.; Schrader, G. L.; Pruski, M. *J. Am. Chem. Soc.* **2002**, *124*, 8435.
(23) Wadsley, A. D. *Acta Cryst.* **1957**, *10*, 261.
(24) Dupre, N.; Gaubicher, J.; Guyomard, D.; Grey, C. P. *Chem. Mater.* **2004**, *16*, 2725.

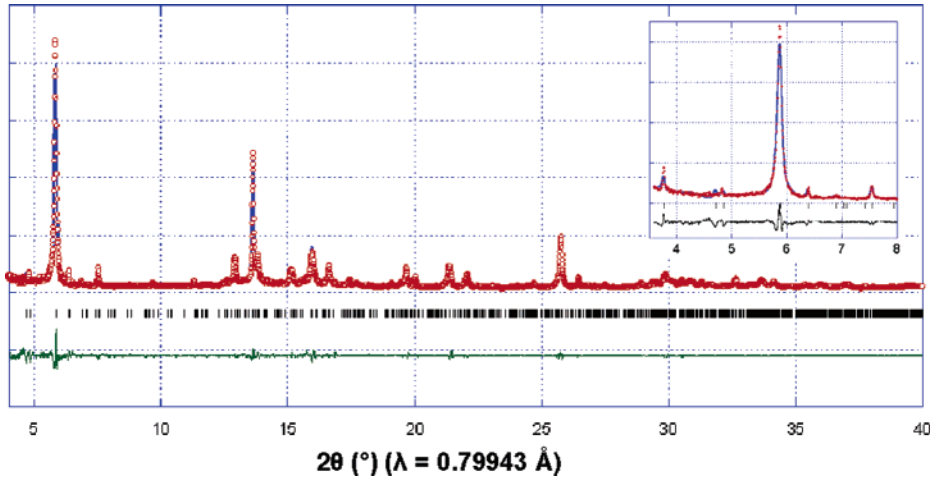

Figure 5. AG90 full pattern matching refinement. A zoom between $2\theta = 3.5°$ and $2\theta = 8°$ is shown in the inset. Circles correspond to the experimental pattern, the full line to that of the calculated one and to the difference curve. Sticks correspond to calculated Bragg positions.

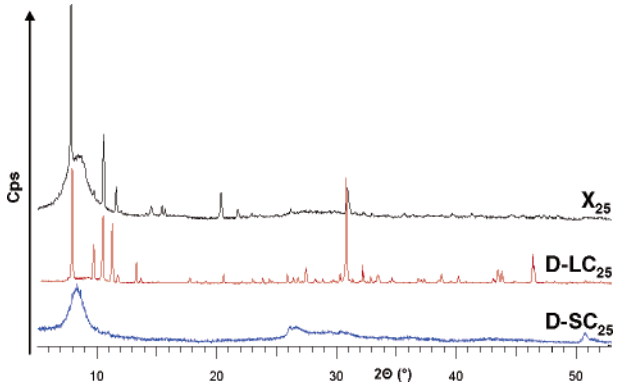

Figure 6. XRD (Cu Kα) patterns of $Li_{1+\alpha}V_3O_8$ GP (X_{25}), its liquid component (D-LC_{25}), and its solid component (D-SC_{25}) extracted from the gel and dried at room temperature.

and small chemical shift anisotropy (CSA) ($\eta_{CSA} = 0.1$ and 0.5 respectively, with a CSA $\sigma_{ani} = \sim 500$ ppm) were found. This assignment is also consistent with the chemical shifts observed for V_2O_5-related compounds, containing vanadium in square pyramids. The two remaining signals at −535 and −550 ppm were then assigned to the two octahedral sites. The severe overlap of the two resonances prevented an accurate determination of the CSA and quadrupole coupling parameters. On the basis of these results, it is possible to assign the intense resonance at −545 ppm in the D-SC_{25} spectrum to vanadium in octahedral sites. No resolution of the different octahedral environments that might be present could be achieved, by using either single-pulse or echo sequences, due to the large line width of the resonance. However, deconvolution and integration of the intensities from the spectrum obtained at 4.7 T, using a single-pulse experiment yielded a ratio of 2.3/3 for the signal at −545 ppm with respect to the total signal. This is consistent with 2 vanadium ions out of 3 being on the octahedral site, considering the accuracy of these deconvolutions. In addition, to get a very rough estimate of the quadrupole coupling constant (Q_{cc}) for the octahedral sites, a simulation of the signal at −545 ppm was performed, using the Simpson[11] program. These simulations were performed on the spectrum obtained from the Hahn-echo experiment due to their slightly better resolution. The following results are provided so as to illustrate the differences in the distortions of the different

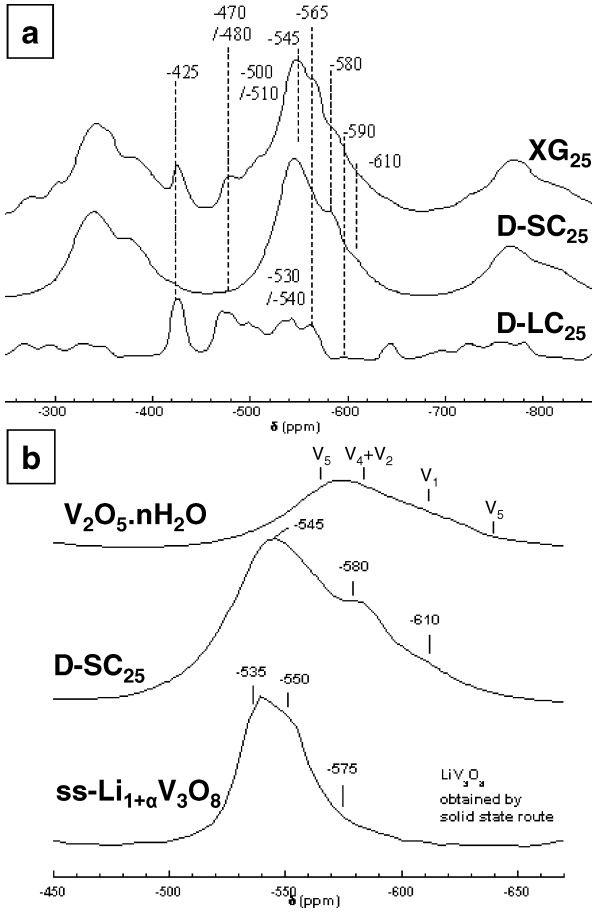

Figure 7. (a) ^{51}V MAS NMR spectra showing the isotropic resonances of X_{25}, D-SC_{25}, and D-LC_{25}, acquired at $B_0 = 8.4$ T, $\nu_r = 20$ kHz. (b) ^{51}V MAS NMR spectra showing the isotropic resonances of D-SC_{25}, ss-$Li_{1.1}V_3O_8$ obtained by a solid-state route, and xerogel of V_2O_5, acquired at $B_0 = 8.4$ T, $\nu_r = 20$ kHz, except for $Li_{1.1}V_3O_8$ ($\nu_r = 15$ kHz). The nomenclature used for the different vanadium environments in $V_2O_5 \cdot nH_2O$ is from ref 21.

local environments, since we believe that the −545 ppm resonance most likely contains two overlapping signals due to the octahedral vanadium ions. In particular, the relative orientation of the electric field gradient and chemical shift tensors could not be determined. The resonance at −545 ppm is associated with a quadrupole coupling constant of 1.5 MHz a with large value of the asymmetry parameter ($\eta_Q = 0.8$)

and with a small CSA of below 500 ppm ($\eta_{CSA} = 0.2$). In comparison, the quadrupole coupling constant increases to 2.0 MHz for the resonance at −580 ppm, the other parameters remaining unchanged, consistent with the increase in Q_{cc}, from octahedral to pentacoordinated configuration, seen previously in the study of $Li_{1+x}V_3O_8$.[24] These results support the assignments of the signals at −545 and −580 ppm to octahedral and square-pyramid sites, respectively. The sideband manifold of the signal at −610 ppm could be fitted with parameters close to those found for pentacoordinated vanadium in a chain configuration in V_2O_5 gels[22] but with a slightly higher value for quadrupole coupling asymmetry parameter ($\eta_Q = 0.7$) and an asymmetry parameter different from 0, supporting the analogy with the square-pyramid environments found in V_2O_5 along with a higher degree of distortion. Thus, it clearly appears from these results that the local structure of the D-SC_{25} sample is different from that of a V_2O_5 gel and already contains vanadium in octahedral and square-pyramid local environments similar to those found in $Li_{1.0}V_3O_8$ and $Li_{1.1}V_3O_8$.

In concern of the D-LC_{25} sample (Figure 7a), most of the observed resonances, in particular at −425, −500, −510, and −530 ppm, can be assigned to vanadium in decavanadic acid.[25,26] Resonances in the range of −540/−575 ppm are usually attributed to vanadate ($[VO_2]^+$) or polyvanadate ($[VO_4]^{3-}$, $[(VO_3)_x]^{x-}$, $[V_4O_{12}]^{4-}$) ions. Resonances between −575 and −590 ppm are observed in V_2O_5 gel and correspond to vanadium in square-pyramid environments with a structural water molecule weakly bonded to the vanadium atom or to the apical oxygen.[22] Shifts of −470 and −480 ppm have not been observed in previous studies of vanadium species in solution but appear in the same range of frequencies as the solution species and can, therefore, either be assigned to a local environment close to that of decavanadic acid or to precipitates from Li^+ ions and polyvanadate species. As a consequence, D-LC_{25} consists predominantly of decavanadic acids and polyvanadic species, as opposed to D-SC_{25}. Moreover, no detectable signal at lower frequencies, between −600 and −620 ppm, could be observed, even using higher spinning speed, indicating the absence of V_2O_5-like environments. Thus, the D-LC_{25} and D-SC_{25} compounds are structurally quite different from V_2O_5 gels.

All the resonances seen in the spectra of these two samples are found in that of X_{25}, X_{25} being clearly the sum of D-LC_{25} and D-SC_{25} spectra (Figure 7a).

The spectra of the D-LC_{90} sample are dramatically different (Figure 8) as a resonance at −585 ppm corresponding to a square-pyramid environment and broad signals at −520 and −555 ppm that are close to the resonances seen at −535 and −550 ppm on the spectrum of ss-$Li_{1.1}V_3O_8$ are seen. The signals at −520 and −555 ppm can be tentatively assigned to the two octahedral sites of $Li_{1.1}V_3O_8$. This result confirms that D-LC_{90} heated at 90 °C is structurally related to $Li_{1.1}V_3O_8$, consistent with the transformation of the former into LVOH1 (Figure 8).

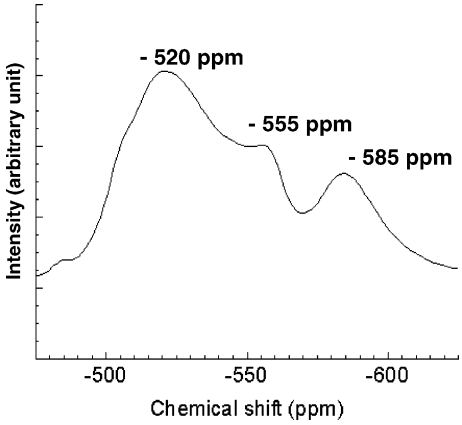

Figure 8. An enlargement of the ^{51}V MAS NMR spectra of D-LC_{90} acquired at $B_0 = 8.4$ T, $\nu_r = 15$ kHz, showing the isotropic resonances.

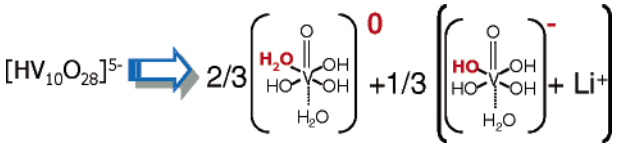

Figure 9. Proposed intermediate species stable at pH 4.2 that would be involved in the condensation mechanism of the $Li_{1+\alpha}V_3O_8$ GP according to partial charge calculation.

A condensation mechanism of the V_2O_5 gel at pH 2 has been proposed by J. Livage;[16] it implies a neutral precursor $[VO(OH)_3(OH_2)_2]^0$. Layered solid phases are currently obtained upon thermohydrolysis around pH 7, and it has been assumed that anionic precursors such as $[VO(OH)_4(OH_2)]^-$ could be involved in the formation of the vanadium oxide.[27] Partial charge calculation using the Marc Henry model[28] shows that in the case of the $Li_{1+\alpha}V_3O_8$ GP formed at pH 4.2, i.e., at a slightly higher value than the point of zero charge (pH 2), a mixture of the hypothetical neutral $[VO(OH)_3(OH_2)_2]^0$ and of the anionic $[VO(OH)_4(OH_2)]^-$ precursors with a 2/1 ratio respectively is involved in the condensation process (Figure 9). It can be assumed that olation and oxolation reactions lead to the $V_3O_8^{(1+\alpha)-}$ network that precipitates in the presence of Li^+ ions to give the hydrated oxide $Li_{1+\alpha}V_3O_8 \cdot 3H_2O$ (LVOH3).

Discussion

In short, previous results show that the gelation pH of $Li_{1+\alpha}V_3O_8$ is close to 4 vs 2 for the V_2O_5 gel. Moreover, coupled XRD and NMR results strongly suggest that the solid part shows the hewettite $Li_{1+\alpha}V_3O_8$ type structure. The structural discrepancies of the $Li_{1+\alpha}V_3O_8$ and V_2O_5 gels could arise from the nature of the V(V) solute precursors in solution. These would be only neutral precursors $[VO(OH)_3(OH_2)_2]^0$ at pH 2 vs neutral and negative precursors at pH 4.2. On this basis, we would like to propose in the following a mechanism that would account for the condensation of the $Li_{1+\alpha}V_3O_8$-type structure contained in the gel (LVOH3) from these solute species. Such a mechanism is strictly speculative and is mainly an attempt to understand reactions that occur in solution, but we believe that, in a way, it fairly supports

(25) Harrison, A. T.; Howarth, O. W. *J. Chem. Soc., Dalton Trans.* **1985**, 1173.
(26) O'Donnell, S. E.; Pope, M. T. *J. Chem. Soc., Dalton Trans.* **1976**, 2290.
(27) Chirayil, T.; Zavalij, P. Y.; Whittingham, M. S. *Chem. Mater.* **1998**, *10*, 2629.
(28) Henry, M.; Jolivet, J. P.; Livage, J. *Structure Bonding* **1992**, *77*, 153.

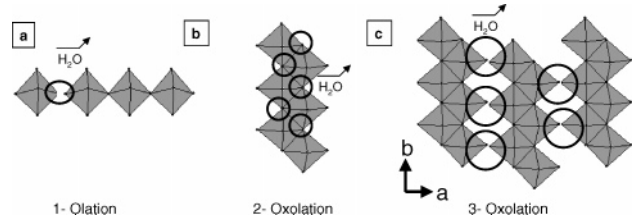

Figure 10. V_2O_5 gel condensation mechanism in 3 steps as proposed in a previous work.[16]

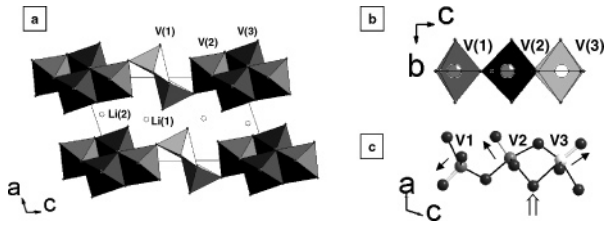

Figure 11. (a) View of the $Li_{1+\alpha}V_3O_8$ structure along [010] and (b) the three vanadium sites along [100] and (c) along [010].

the contribution of the pH on the structural type that condenses. As it is provided further down, our approach got its footing with thorough observations of structural features that are specific to $Li_{1+\alpha}V_3O_8$.

First of all, let us remind the hypothetical condensation mechanism that was proposed in a previous work to lead to V_2O_5 gel.[16] The V_2O_5 gel network presents edge and corner sharing squared pyramids (Figure 10c). The neutral precursor is composed of three hydroxo and one aquo ligands in the equatorial plane allowing olation and oxolation condensation mechanisms.[16] Figure 10 presents the three major steps of the condensation mechanism of V_2O_5 gel as described in the literature.[16] The first step consists of the formation of a chain composed of corner-linked octahedra via an olation mechanism (Figure 10a). It is followed by connection of two such chains via oxolation (Figure 10b) giving rise to a ribbon of edges-linked octahedra. The next would correspond to the formation of corrugated double layers via an oxolation reaction as observed in V_2O_5 xerogel structure (Figure 10c). In the case of the negatively charged precursor that is present when $V_3O_8^{(1+\alpha)-}$ layers form, only apical H_2O ligands can condense via olation.

Figure 11a shows the structure of $Li_{1+\alpha}V_3O_8$ along the *b* axis. Three vanadium sites (noted V(1), V(2), and V(3)) and two lithium sites (noted Li(1) and Li(2)) are present. A closer look at the chains of vanadium ions shows that the double chain related to V(1) (square-pyramid site) is similar to that in the V_2O_5 gel, whereas the quadruple chain (V(2)−V(3)) (octahedral site) is specific to $Li_{1+\alpha}V_3O_8$ as the respective orientation of vanadyl bonds V═O is different from that observed in the V_2O_5 gel. The presence of these two types of V chains leads us to consider two groups of reactions. The first one would drive to V(1) double chains as in V_2O_5 gel and consequently would only involve neutral precursors. In this condition, in the second group the formation of the quadruple chains V(2)−V(3) would stem from condensation of the remaining neutral and negative precursors as well as Li^+ ions.

Moreover, Figure 11b shows that the three vanadyl bonds (all V polyhedra appear as octahedral for the sake of clarity)

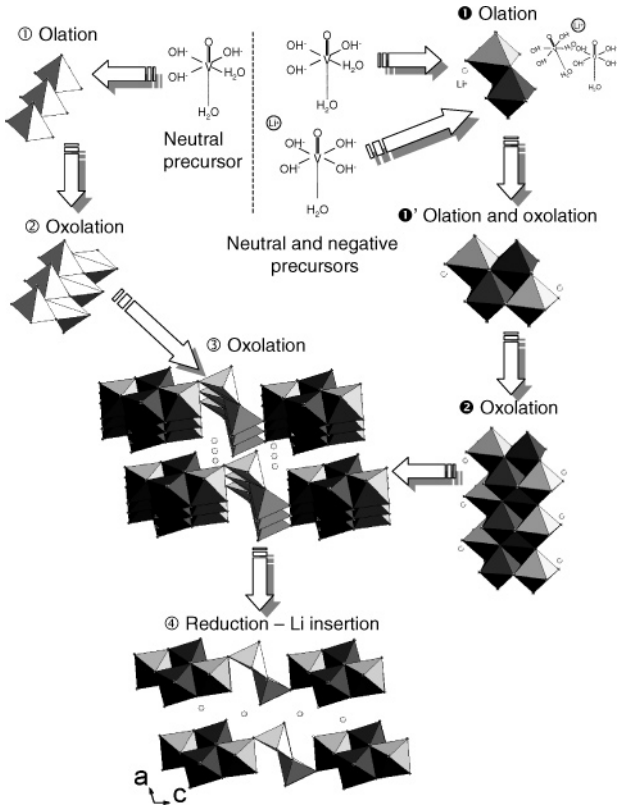

Figure 12. Proposed mechanism for the condensation of $Li_{1+\alpha}V_3O_8$.

lie in the same plane (a and c) and that they are perpendicularly oriented in a sequence that can be schematized as ←↑→ for V(1), V(2), and V(3), respectively (Figure 11c). Such a sequence implies a bond between two apical O atoms (pointed by an arrow in Figure 11c. Consequently and as opposed to reactions that should occur in the first group (V(1)), in the second group, the apical V−OH_2 bond of the precursors should participate to the condensation mechanism.

According to these observations regarding the structure of $Li_{1+\alpha}V_3O_8$, a hypothetical mechanism can be proposed for the condensation of the solid component of the gel (LVOH3). This mechanism has been divided into five steps, as summarized in Figure 12.

The first group of reactions that is associated to one of the two neutral precursors gives rise to V(1) double chains upon olation (step 1, left) and oxolation (step 2, left) reactions,[16] as for V_2O_5. In the second group, the two vanadium precursors can form edge-sharing dimers via an olation reaction (step 1, right) where Li^+ ion would help the two precursors to orient themselves such as apical water is involved in the reaction. In most cases,[29] however, olation mechanisms are faster than oxolation ones. Then quadrimers would appear (step 1′, right) via olation and oxolation reactions leading finally to a quadruple chain of octahedra by oxolation (step 2, right). The as-formed quadruple chain corresponds to the V(2)−V(3) chains found in the structure of $Li_{1+\alpha}V_3O_8$ (Figure 11a). At this point, two infinite chains are formed: a double chain V(1) and a quadruple chain V(2)−V(3). These two chains can condense via a last

(29) Jolivet, J. P. De la solution à l'oxyde: Condensation des cations en solution aqueuse, Chimie de surface des oxydes; collection Savoir Actuel, InterEditions/CNRS éditions 1994.

oxolation reaction (step ③) leading theoretically to $Li_{1.0}V_3O_8$.

$Li_{1.0}V_3O_8$ is, however, a very unstable compound in an aqueous medium since the electrochemical oxidation/deinsertion of $Li_{1+\alpha}V^{5+}{}_{3-\alpha}V^{4+}{}_{\alpha}O_8$ to $Li_{1.0}V^{5+}{}_3O_8$ (that corresponds to the removal of α (Li^+,e^-)) can only be completed at high voltage (4.2 V vs Li^+/Li^0, i.e., 1.2 V vs H^+/H_2).[30] As a consequence we believe that, simultaneous to the formation of $Li_{1.0}V_3O_8$ in water, the compound, or an intermediate fragment of the compound, oxidizes partly water and thus is slightly reduced (transfer of α electrons). The charge compensation is probably achieved by α residual lithium ions from the reaction medium migrating into the interlayer space, leading to the final composition $Li_{1+\alpha}V_3O_8 \cdot nH_2O$ (step ④). Note that the α extra Li^+ ions might correspond to those that lie on the tetrahedral Li(2) site observed in the anhydrous $Li_{1+\alpha}V_3O_8$ (Figure 11a).

Conclusion

To conclude, this paper shows that the gelatinous precipitate precursor of $Li_{1+\alpha}V_3O_8$, qualified as a gel in the literature, is actually a biphasic material made of a liquid phase trapped in a porous solid. The latter is a red ill-crystallized hewettite-like layered hydrated phase $Li_{1+\alpha}V_3O_8 \cdot 3H_2O$ with the specific network similar to that of the anhydrous $Li_{1+\alpha}V_3O_8$. It results from the condensation of solute vanadic precursors around pH 4. The condensation of a different structure than that of V_2O_5 gel stems from the presence of both Li^+ ions and the anionic vanadium precursor. The yellow supernatant solution corresponds to solute decavanadate species that precipitate into lithium decavanadates at room temperature. This latter transforms to hydrated hewettite-like $Li_{1+\alpha}V_3O_8 \cdot yH_2O$ ($y \approx 1$) upon drying at 90 °C.

Further work (Part II) will be devoted to structural transformations from the gel-like precursor to anhydrous $Li_{1+\alpha}V_3O_8$. It will be shown that the diphasic character of the xerogel influence the electrochemical behavior.

Acknowledgment. The authors are grateful to M. N. Rager for liquid ^{51}V NMR, J. P. Jolivet and L. Brohan for fructuous discussions, and D. Tastemale for XRD technical assistance at ESRF and SNBL. This work was done with financial support of CNRS and region Pays de la Loire. C.P.G. thanks the National Science Foundation (Grant DMR0211353).

CM047845K

(30) Dupre, N.; Gaubicher, J.; Guyomard, D.; Gray, C. *Chem. Mater.* **2004**, *16* (14), 2725.